

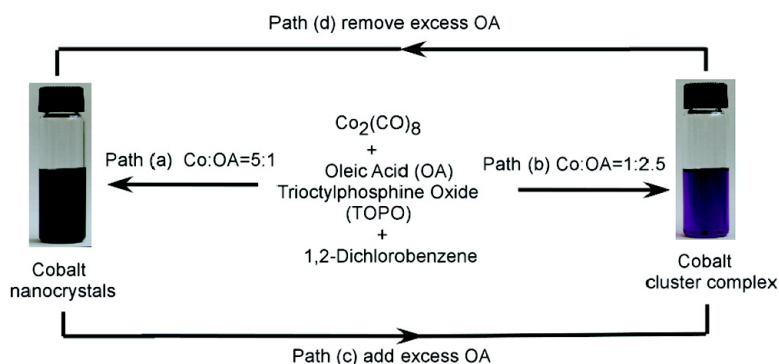
Communication

Ligand Effect on the Growth and the Digestion of Co Nanocrystals

Anna C. S. Samia, Kylee Hyzer, John A. Schlueter, Chang-Jin
 Qin, J. Samuel Jiang, Samuel D. Bader, and Xiao-Min Lin

J. Am. Chem. Soc., **2005**, 127 (12), 4126-4127 • DOI: 10.1021/ja044419r • Publication Date (Web): 03 March 2005

Downloaded from <http://pubs.acs.org> on March 24, 2009



More About This Article

Additional resources and features associated with this article are available within the HTML version:

- Supporting Information
- Links to the 11 articles that cite this article, as of the time of this article download
- Access to high resolution figures
- Links to articles and content related to this article
- Copyright permission to reproduce figures and/or text from this article

[View the Full Text HTML](#)

Ligand Effect on the Growth and the Digestion of Co Nanocrystals

Anna C. S. Samia,[†] Kylee Hyzer,[‡] John A. Schlueter,[‡] Chang-Jin Qin,[§] J. Samuel Jiang,[‡] Samuel D. Bader,^{†,⊥} and Xiao-Min Lin^{*,†,‡,⊥}

Chemistry Division, Materials Science Division, and Center for Nanoscale Materials, Argonne National Laboratory, Argonne, Illinois 60439, and Department of Chemistry, University of Chicago, 5635 South Ellis Avenue, Chicago, Illinois 60637

Received September 14, 2004; E-mail: xmlin@anl.gov

The growth and stability of nanocrystals in organic solvents rely on the presence of stabilizing ligands.¹ Under various kinetic and thermodynamic conditions, monodispersed nanocrystals with controllable sizes, shapes, and chemical compositions have been synthesized recently.² However, the effects of surface ligands, especially how they regulate the growth of nanocrystals, have not been studied thoroughly. The common notion is that Ostwald ripening and coalescence coarsening control the particle growth process after nucleation.³ Thus, a kinetic control process such as “size focusing” is needed to maintain the monodispersity of a growing colloid.⁴ Recent experimental evidences in Au, Ag, and PbS nanocrystal synthesis have shown that the presence of excess ligand in the system could result in a completely different ripening process, namely the growth inhibition or even disintegration of large nanocrystals in favor of smaller particles, a process named digestive ripening.⁵ In this report, we demonstrate that using different concentrations of oleic acid ligand during the cobalt carbonyl decomposition results in the formation of either large nanocrystals or small clusters. More dramatically, we show that by adding or removing free oleic acid ligand from the final reaction product, we can turn a nanocrystal colloid into a cluster complex solution and vice versa.

A general procedure to synthesize cobalt nanocrystals is shown in path (a) of Figure 1, which is a modification of the procedure used by several other groups⁶ (see Supporting Information for detailed description). Nanocrystals are obtained through thermal decomposition of $\text{Co}_2(\text{CO})_8$ in the presence of oleic acid (OA) and a small amount of trioctylphosphine oxide (TOPO), with the Co:OA molar ratio fixed at 5:1. It was found that after a quick injection of precursor at 180 °C and then lowering the growth temperature to 130 °C, nanocrystals will nucleate and grow uniformly. The particle size, which is a function of reaction time, typically reaches 6 nm in diameter after 15 min, and becomes 9.5 nm after 1 h. Figure 2a shows a monolayer of 9.5 nm cobalt nanocrystals after being washed by methanol, redispersed in anhydrous toluene, and then deposited onto a carbon grid. Powder X-ray diffraction (inset of Figure 2a) shows that, different from the face centered cubic (fcc) and hexagonal closed packed (hcp) structures in the bulk cobalt, these particles adopt the ϵ phase, a distorted fcc structure that is only observed in nanocrystals.⁶ Magnetic measurements show the blocking temperature of these large particles is close to room temperature; thus, they are ferromagnetic near room temperature, with their easy axis randomly orientated in the sample (Figure 2b and Figure S4 in Supporting Information). The saturation magnetization was close to the bulk value (Figure S4 in Supporting Information), and no shift of

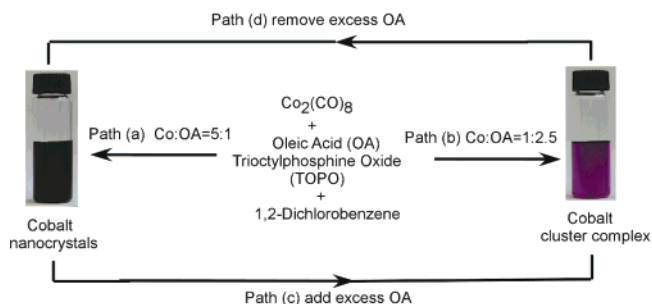


Figure 1. Schematic diagram illustrating the experimental procedures to synthesize cobalt nanocrystals and cluster complexes using different concentrations of oleic acid ligand (see Supporting Information for experimental details.)

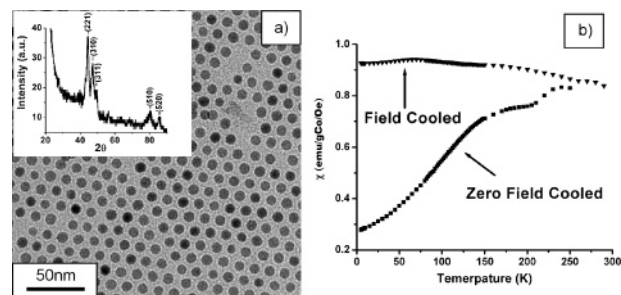


Figure 2. (a) Transmission electron micrograph (TEM) of the as-prepared 9.5 nm Co nanocrystals. (Inset) X-ray powder diffraction showing that the crystal structure of the cobalt is ϵ -phase. (b) Zero-field-cooled (ZFC) and field-cooled (FC) magnetic susceptibility of large particles. Small kink at 250 K of the ZFC curve is attributed to small size nonuniformity of the sample.

hysteresis loop was detected, indicating the absence of a cobalt oxide layer on the nanocrystal surface.

On the other hand, when the same reaction was conducted using a higher concentration of OA (Co:OA ratio of 1:2.5), while keeping all the other conditions the same (path (b) in Figure 1), the result is drastically different. After the $\text{Co}_2(\text{CO})_8$ injection, the color of the reaction mixture turned to black briefly (indicating the initial formation of cobalt nanocrystals) before changing to blue color after 1 h. The rate at which this transition takes place depends on the temperature of the reaction. UV–vis absorption measurement of this solution showed an absorption band in the range of 450–650 nm (inset of Figure 3), with optical transitions between discrete energy levels visible in the spectrum. Electrospray ionization mass spectroscopy (ESI-MS) data were collected using methanol or ethanol as a carrier solvent and under various fragmentation voltages (Figure 3 and Figure S1 in supporting materials). The five groups of predominant ions detected centered near 990 Da. The isotope pattern indicates that these are all +1 charged ions with mass corresponding to clusters of Co_2 and Co_3 coordinated with three

[†] Chemistry Division, Argonne National Laboratory.

[‡] Materials Science Division, Argonne National Laboratory.

[⊥] Center for Nanoscale Materials, Argonne National Laboratory.

[§] Department of Chemistry, University of Chicago.

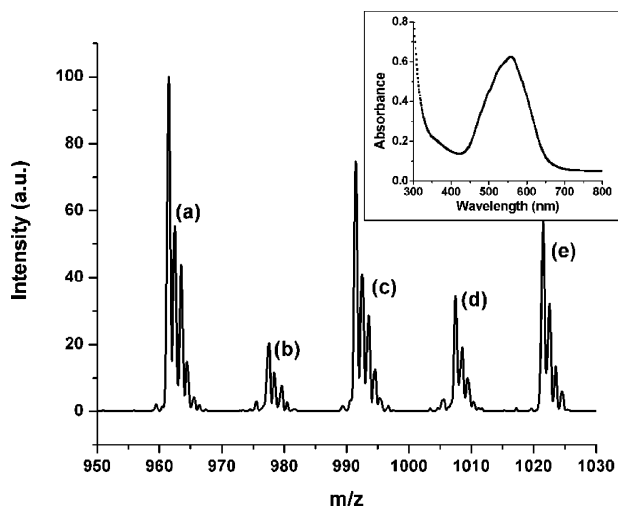


Figure 3. ESI-MS spectrum of the cobalt cluster complex in 1,2-dichlorobenzene at the fragmentation voltage of 200 V, using methanol as a carrier solvent. The mass of the peaks correspond to (a) $[\text{Co}(\text{II})_2(\text{C}_{18}\text{H}_{33}\text{O}_2)_3]^+$, (b) $[\text{Co}(\text{II})_2(\text{C}_{18}\text{H}_{33}\text{O}_2)_3\text{O}]^+$, (c) $[\text{Co}(\text{I})_2(\text{C}_{18}\text{H}_{33}\text{O}_2)_3\text{CO}+2\text{H}]^+$, (d) $[\text{Co}(\text{I})_2(\text{C}_{18}\text{H}_{33}\text{O}_2)_3\text{OCO}+2\text{H}]^+$, (e) $[\text{Co}(\text{I})_3(\text{C}_{18}\text{H}_{33}\text{O}_2)_3+\text{H}]^+$. (Inset) UV-vis absorbance of the cluster solution.

OA ligand molecules. The cobalt centers in these ions have two different valence states. Since the electrospray is a soft ionization technique that creates very little fragmentation,⁷ the clusters we detected most likely exist in the solution.

Intrigued by the very different reaction products under different amount of OA ligand, we carried out experiments shown in paths (c) and (d) of Figure 1. In path (c), Co nanocrystals made from reaction path a were precipitated and washed with anhydrous methanol and redispersed in 1,2-dichlorobenzene. Elemental analysis of the precipitated sample indicates there is a monolayer coating of OA on the particle surface. Excess OA was then added to increase the molar ratio of Co:OA to 1:2.5. The solution was then heated under reflux at 180 °C. Following this step, the black color of the colloidal solution gradually turned blue after 5 h, indicating the disintegration of the large ferromagnetic nanocrystals. Mass spectroscopy data confirmed the formation of the same cluster complex, as shown in Figure 3.

Removal of the excess OA from the cluster complex solution (Figure 1 path (d)) was achieved through reacting the complex solution with lithium aluminum hydride (LAH), a standard reaction that forms lithium aluminum carboxylate salt. LAH also reduce the cobalt ions back to zero valence state. After the LAH injection, the solution changed to black almost instantaneously. Upon removal of the reaction side products through centrifugation, the cobalt nanocrystals were isolated by precipitation with ethanol and confirmed by TEM measurement.

The formation of either large nanocrystals or small cluster complexes under different concentration of OA ligand, and the fact that they can be reversibly interchanged by varying the free ligand concentration, indicate that there is a strong and yet reversible binding between the OA ligand and the Co nanocrystal surface. With the presence of a high concentration of OA ligand, cluster complexes are more stable than large nanocrystals. The dramatic digestive ripening process (path (c)) in which excess OA ligands literally pull Co atoms off the nanocrystal surface to form clusters is a thermodynamically driven process. The similar ripening process in gold-dodecanethiol colloids results in 5–7 nm particles at 120 °C⁵ and small clusters at 300 °C.⁸ In comparison, cluster complexes form at a much lower temperature in the Co–OA system due to the different strengths of the metal–metal and the metal–

ligand bonds. The binding between the ligand and metal surface, however, is a dynamic process. Reducing the concentration of free ligand (in path (d) by reacting it with LAH) will shift the equilibrium, which lowers the concentration of the surface ligand molecules and allows clusters to sinter and eventually form large particles through Ostwald ripening and coalescence coarsening. The fact that Co_2 and Co_3 clusters are possible intermediate building blocks for constructing large nanocrystals may explain why ϵ phase rather than fcc or hcp phase is observed in these syntheses.

The formation of clusters under high concentration of OA is not limited to cobalt. Thermal decomposition of $\text{Fe}(\text{CO})_5$ under identical conditions (Fe:OA molar ratio of 1:2.5) form Fe_1 , Fe_2 clusters (Figure S2 in Supporting Information). However, reducing platinum acetylacetonate with 1,2-hexandecanediol under the same conditions leads to the formation of bulk Pt precipitation. This was also confirmed by results from Weller's group.⁹ Therefore, Pt has a much weaker interaction with OA than Co or Fe. Interestingly, when the thermal decomposition of $\text{Fe}(\text{CO})_5$ occurs in the same solution where platinum acetylacetonate is being reduced (metal: OA = 1:2.5), stable FePt nanocrystals with diameter about 5 nm form.¹⁰ This indicates that it is the formation of alloys between Fe–OA clusters and growing Pt particles that provides a stabilization mechanism for FePt nanocrystals. The relative strength of the ligand–metal and metal–metal interaction can thus regulate the growth of metal and their alloy particles, such as Co, CoPt, and FePt, and in some cases lead to conditions wherein the traditional ripening processes do not occur.

Acknowledgment. We are grateful to Yuping Bao and Kannan Krishnan for the help on initial experiments and Chris Sorensen for many valuable discussions. This work is supported by DOE, BES-Materials Sciences, under Contract W-31-109-ENG-38, and the University of Chicago-ANL Consortium for Nanoscience Research (CNR).

Supporting Information Available: Synthesis procedures, additional TEM images, ESI-MS, and magnetic data. This material is available free of charge via the Internet at <http://pubs.acs.org>.

References

- (1) Schmid, G., Eds. *Clusters and Colloids: From Theory to Applications*; VCH: New York, 1994.
- (2) (a) Murray, C. B.; Kagan, C. R.; Bawendi, M. G. *Annu. Rev. Mater. Sci.* **2000**, *30*, 545–610. (b) Lee, S.-M.; Jun, Y.-w.; Cho, S.-N.; Cheon, J. *J. Am. Chem. Soc.* **2002**, *124*, 11244–11245. (c) Song, Q.; Zhang, Z. *J. Am. Chem. Soc.* **2004**, *126*, 6164–6168. (d) Jana, N. R.; Gearheart, L.; Murphy, C. J. *J. Phys. Chem. B* **2001**, *105*, 4065–4067. (e) Peng X. A. Peng, X. *J. Am. Chem. Soc.* **2001**, *123*, 1389–1395. (f) Manna, L. Scher, E. C.; Alivisatos, A. P. *J. Am. Chem. Soc.* **2000**, *122*, 12700–12706.
- (3) Ratke, L.; Voorhees, P. W. *Growth and Coarsening*; Springer-Verlag: Berlin, 2002.
- (4) Peng, X. G.; Wickham, J.; Alivisatos, A. P. *J. Am. Chem. Soc.* **1998**, *120*, 5343–5344.
- (5) (a) Lin, X. M.; Sorensen, C. M.; Klabunde, K. J. *J. Nanopart. Res.* **2000**, *2*, 157–164. (b) Prasad, B. L. V.; Stoeva, S. I.; Sorensen, C. M.; Klabunde, K. J. *Chem. Mater.* **2003**, *15*, 935–942. (c) Stoeva, S.; Klabunde, K. J.; Sorensen, C. M.; Dragieva, I. *J. Am. Chem. Soc.* **2002**, *124*, 2305–2311. (d) Smetana, A. B.; Klabunde, K. J.; Sorensen, C. M. To be published. (e) Hines, M. A.; Scholes, G. D. *Adv. Mater.* **2003**, *15*, 1844–1849.
- (6) (a) Puentes, V. F.; Krishnan, K. M.; Alivisatos, A. P. *Science* **2001**, *291*, 2115–2117. (b) Sun, S. H.; Murray, C. B. *J. Appl. Phys.* **1999**, *85*, 4325–4330. (c) Dinega, D. P.; Bawendi, M. G. *Angew. Chem., Int. Ed.* **1999**, *38*, 1788–1791.
- (7) Johnson, B. F. G.; McIndoe, J. S. *Coord. Chem. Rev.* **2000**, *200*–202, 901–932.
- (8) Jin, R. C.; Egusa, S.; Scherer, N. F. *J. Am. Chem. Soc.* **2004**, *126*, 9900–9901.
- (9) Shevchenko, E. V.; Talapin, D. V.; Schnablegger, H.; Kornowski, A.; Festino, O.; Svedlindh, P.; Haase, M.; Weller, H. *J. Am. Chem. Soc.* **2003**, *125*, 9090–9101.
- (10) Chen, M.; Liu, J. P.; Sun, S. *J. Am. Chem. Soc.* **2004**, *126*, 8394–8395.

JA044419R